An electrical-heating and self-sensing shape memory polymer composite incorporated with carbon fiber felt

2016 Smart Mater. Struct. 25 035036

(http://iopscience.iop.org/0964-1726/25/3/035036)

IOP Publishing Smart Materials and Structures
Smart Mater. Struct. **25** (2016) 035036 (10pp) doi:10.1088/0964-1726/25/3/035036

An electrical-heating and self-sensing shape memory polymer composite incorporated with carbon fiber felt

Xiaobo Gong[1], Liwu Liu[2], Yanju Liu[2] and Jinsong Leng[1]

[1] Centre for Composite Materials and Structures, Harbin Institute of Technology, Harbin HIT Science Park, No. 2 YiKuang Street, Harbin, 150080, People's Republic of China
[2] Department of Astronautical Science and Mechanics, Harbin Institute of Technology PO Box 301, No. 92 West Dazhi Street, Harbin 150001, People's Republic of China

E-mail: lengjs@hit.edu.cn

Received 25 August 2015, revised 10 December 2015
Accepted for publication 18 January 2016
Published 22 February 2016

Abstract

Shape memory polymers (SMPs) have the ability to adjust their stiffness, lock a temporary shape, and recover the permanent shape upon imposing an appropriate stimulus. They have found their way into the field of morphing structures. The electrically Joule resistive heating of the conductive composite can be a desirable stimulus to activate the shape memory effect of SMPs without external heating equipment. Electro-induced SMP composites incorporated with carbon fiber felt (CFF) were explored in this work. The CFF is an excellent conductive filler which can easily spread throughout the composite. It has a huge advantage in terms of low cost, simple manufacturing process, and uniform and tunable temperature distribution while heating. A continuous and compact conductive network made of carbon fibers and the overlap joints among them was observed from the microscopy images, and this network contributes to the high conductive properties of the CFF/SMP composites. The CFF/SMP composites can be electrical-heated rapidly and uniformly, and its' shape recovery effect can be actuated by the electrical resistance Joule heating of the CFF without an external heater. The CFF/SMP composite get higher modulus and higher strength than the pure SMP without losing any strain recovery property. The high dependence of temperature and strain on the electrical resistance also make the composite a good self-sensing material. In general, the CFF/SMP composite shows great prospects as a potential material for the future morphing structures.

Keywords: shape memory composite, carbon fiber felt, electrical-heating, self-sensing, morphing structures

(Some figures may appear in colour only in the online journal)

1. Introduction

As typical smart materials, shape-memory polymers (SMPs) have the features of changeable shape and variable stiffness. They can be changed and fixed into a temporary shape from a permanent shape, and then recover their permanent shape upon applying an appropriate stimulus [1]. The SMPs develop rapidly in recent years, due to their superior structural versatility, low density, low cost, high elastic deformation, and low recovery temperature [2, 3]. These unique characteristics make them be used in a myriad of fields, including clothing manufacturing, deployable space structures , morphing aircraft, medical treatment, and many other applications [4].

In the previous engineering research, an element composed of a set of nichrome wires or kapton heater film was used to activate the SMP by electric resistance heating, but the heat distribution was not adequately uniform [5–7]. The wire diameter was close to the thickness of the skin, which will cause divots along the wire and, they would break over several cycles [5]. The electrically Joule resistive heating of the conductive composite can be a desirable stimulus to activate the shape memory effect of SMPs without an external

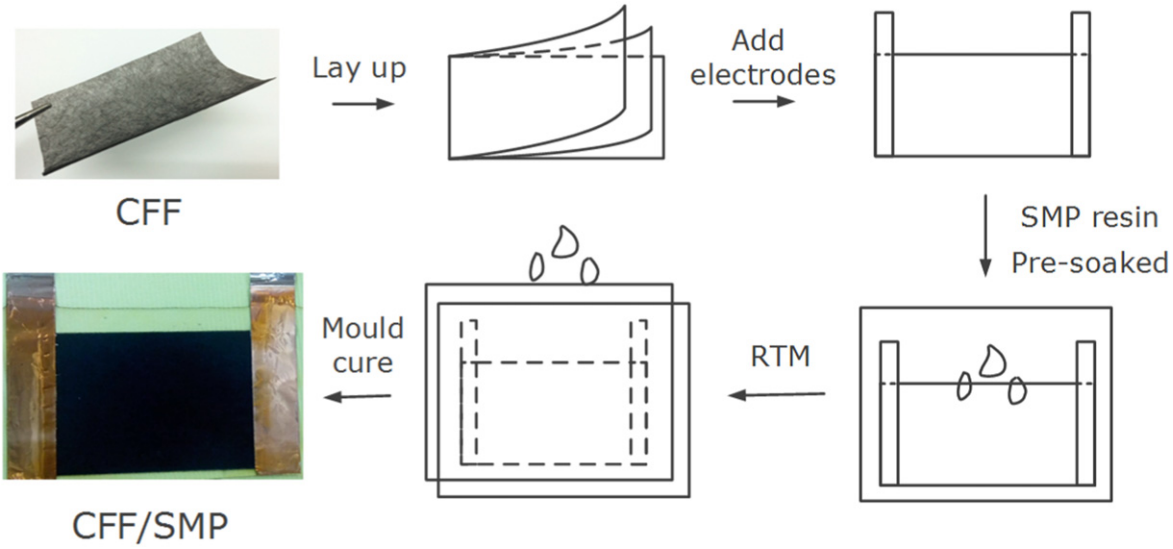

Figure 1. A schematic of the CFF/SMP composite preparation.

heating equipment. Many efforts have been proposed focusing on electrical-heating SMP composites by involving conductive materials. These composites can be activated without an external heater. We divide these conductive material into three categories: (1) discrete fillers [8–10], such as carbon nanotubes [11–14], graphene [15], carbon particles [16–18], hybrid conductive fiber [17, 19], and ferromagnetic particles [20, 21], etc; (2) carbon nanopaper [22] made from carbon nanotubes or carbon nanofibers; (3)continuous carbon fiber [23]; (4) conductive polymer [24, 25]. These composites can achieve low resistivity and be electro-activated without an external heater. For example, the resistivity of composite with 5 wt% multiwall carbon nanotube is $10^3\,\Omega$ cm [11], that of composite with 2.38 wt% carbon powder is 10^4–$10^5\,\Omega$ cm [18], that of composite with 2.63 wt% vapor grown carbon nanofiber is $5 \times 10^2\,\Omega$ cm [19], that of composite with 5 wt% carbon nanopaper is $10^3\,\Omega$ cm [22], that of composite with 6–20 wt% polypyrrole is $10^2\,\Omega$ cm [24], that of composite with 27 wt% continuous carbon fiber is $10^{-3}\,\Omega$ cm [23, 26]. Compared with the SMP composite incorporated with discrete fillers, carbon nanopaper and conductive polymer, the CFF/SMP composite (in this work) with 2.7 wt% CFF has a lower resistivity, 2.019 Ω cm, contributing to an excellent electrical hearting property. Compared with the composite incorporated with continuous carbon fiber, our CFF/SMP composite could avoid the extremely low resistivity which may cause the local overheating problem around the electrode [23].

On the other hand, for the SMP composite filled with discrete fillers, it is difficult to disperse the fillers homogeneously. To obtain satisfactory electrical conductivity, a much higher filler loading is required, which may result in unacceptable mechanical properties, high densities, processing difficulties and high costs [15]. As to the composite with carbon nanopaper, carbon nanopaper costs too much on its raw materials and the complicated manufacture process. Furthermore, the carbon nanopaper are brittle, which could hardly improve the mechanical properties of the composite, while inversely reduce the elongation.

In this paper, an electro-induced shape memory polymer (SMP) composites incorporated with carbon fiber felt (CFF) were manufactured and investigated. The CFF/SMP composite can be electrical-heated rapidly and homogeneously resulting from high electrical conductivity and enhanced heat transfer efficiency. The investigations were focused on the microstructure morphology, mechanical properties, electrical conductivity, shape recovery behaviors, heating performance, tunable temperature distribution, and temperature and strain sensing abilities.

2. Fabrication of CFF/SMP composites

2.1. Material

The epoxy-based SMP used in this work was a thermoset consisting three parts, the epoxy resin, the curing agent, and a linear monomer [27]. The linear monomer is composed of a long linear chain of C–O bonds. The epoxy base resin and the linear monomer have an epoxy group number ratio of 1:1 in one molecule, a molecular weight ratio of 2:5 and a density ratio of 1:1. The epoxy resin and hardener were mixed in a ratio of 1:1. And 5 wt% active linear epoxy monomer is copolymerized with the polymer matrix to adjust its molecular structure. The CFF was purchased from the Kaifeng Pengyuan Glassfiber Products Co. Ltd, and it is a non-woven tissue made of randomly oriented carbon fibers. The carbon fibers are distributed in a special binder through a wet lay process. The CFF has the surface density of $10\,\mathrm{g\,m^{-2}}$, filament diameter of $7.02 \pm 2\,\mu$m, organic matter content of less than 5 wt%, and carbon fiber tensile modulus of 207 GPa.

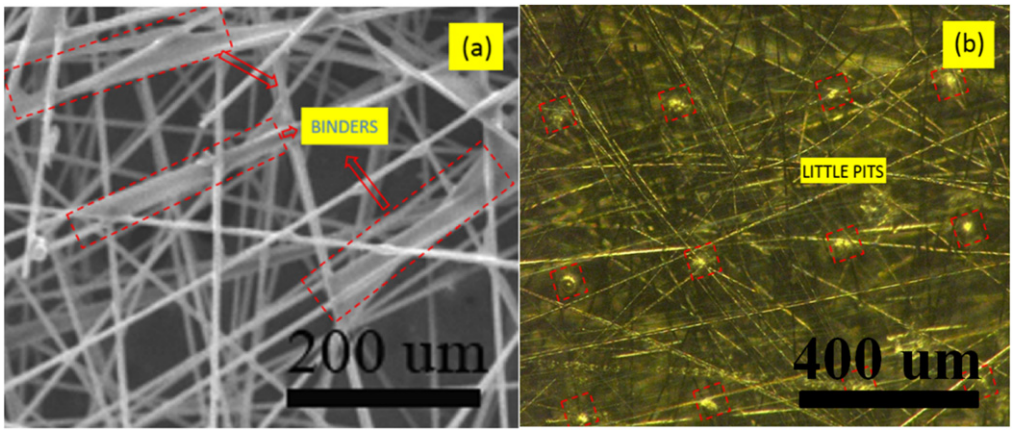

Figure 2. (a) Scanning electron microscopy image of CFF, the scale bar is 200 μm. (b) Optical microscope image of CFF/SMP composite at a magnification of 200×. The bright yellow areas represent the resin. The light points on the composite surface are little pits result from the mould releasing cloth.

2.2. Preparation of CFF/SMP composite

Resin transfer moulding process was used to make the CFF/SMP composite (figure 1). The CFF was cut into rectangles with the dimension of 100 × 65 mm^2, then these rectangular layers were piled up to achieve different weight ratio in the composite. The CFF laminates containing 0, 1, 2, 3, and 4 layers of CFFs corresponds to a CFF mass fractions of 0%, 0.9%, 1.8%, 2.7% to 3.6%, respectively. Subsequently, the electrodes made of copper foil were overlapped 10 mm with the CFF surface and adhered to it with conductive nanosilver glue (HS-100RF, Kunshan Hisense Electronic Co., Ltd). To get a tight conductive connection, the CFFs with electrodes was heated at 135 °C for 1 h to cure the glue. Then the CFF laminates with electrodes were pre-soaked with the SMP resin in the mould for 2 h at room temperature to make the resin penetrate into the interior of the CFF and make sure each carbon fiber was enwrapped by the SMP resin. After the pre-soaking process, the mould was clamped, then the SMP resin was injected into the mould. The resulting mixture was degassed in a vacuum atmosphere for 40 min. Finally, the mixture composited with CFFs and epoxy-based SMP was moulding cured in an oven according to the following process: 80 °C for 3 h, 100 °C for 3 h, and 150 °C for 5 h. The obtained CFF/SMP composite laminate has a thickness of 1 mm.

3. Results and discussion

3.1. Morphology and structure of CFF and CFF/SMP composite

The morphology and structure of CFF were characterized by a scanning electron microscopy (SEM) at an accelerated voltage of 30.0 kV. As shown in figure 2(a), the carbon fibers are randomly oriented and crossovers among the fibers exist in the whole felt. The carbon fibers and the crossovers among them result in a conductive network for electrons in the CFF. This network will contribute to form a low and homogeneous electric resistance, which will be discussed in the following section. We also note that carbon fibers are interconnected with each other by the binders in the CFF. The binders integrate the random carbon fibers and make them a felt, at the same time they have little influence on the whole resistance because of the low content and the existence of the electron tunnelling effect [8, 28]. Figure 2(b) is an optical image at 200× magnification captured by a KEYENCE (VH-Z500R) microscope system. It reveals that the SMP resin evenly impregnates throughout the CFFs, and the conductive network made of carbon fibers and crossovers among them stays unchanged in the composite. The overlap joints among carbon fibers observed from the SEM and the optical microscope images confirm that a continuous conductive network has been established in the CFF/SMP composite.

3.2. Electrical resistivity measurement

The electrical resistivity of CFF and its shape memory composite can be calculated from the following equation,

$$\rho = \frac{R \cdot S}{L},$$

where ρ is the electrical resistivity, R is the electrical resistance, and L, S are the length and cross-sectional area. R was obtained by measuring the electrical resistance between the two electrodes using a digital multimeter (Tektronix) with two-point method. The electrical resistivity of CFF and their composites are plotted versus different mass fractions (figure 3). The error bar represents a standard deviation to demonstrate the variability in electrical resistivity of each three test samples. Comparing the electrical resistivity of CFF and CFF/SMP composite, we could find that the electrical resistivity of CFF/SMP composite is relatively higher than that of pristine CFF. The interfacial effect between the SMP matrix and the carbon fibers were taken into account to explain these phenomena. When the liquid SMP resin was injected in to the CFF, the resin would infiltrated into the gap between the carbon fibers and enwrapped them, and some of the overlap joints among carbon fibers would be weakened or even destroyed due to the introduction of the SMP resin. This

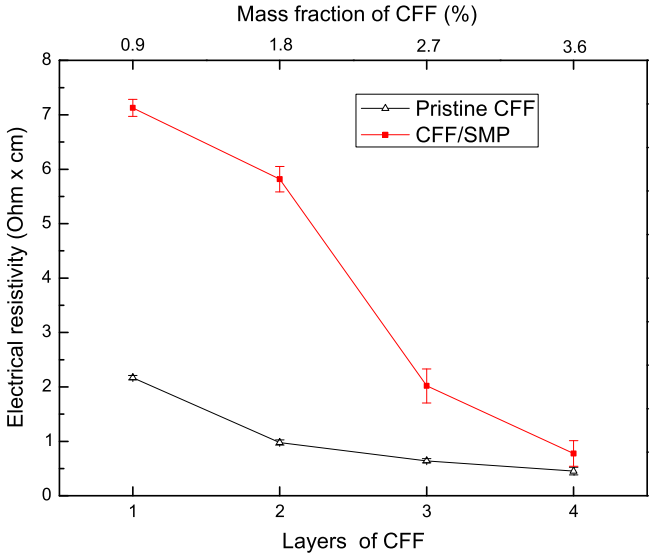

Figure 3. Electrical resistivity of pristine CFFs and CFF/SMP composite.

state would maintain after the curing process, so the electrical resistivity of CFF/SMP composite is much higher than that of pristine CFF.

As to the pristine CFF, with the felts increasing from one layer to four layers, viz., the surface density increasing from 10 to 40 g m^{-2}, the average electrical resistivity decrease gradually from 2.169, 0.979, 0.642 to 0.454 Ω cm. And as to the CFF/SMP composite, with the felts increasing from one layer to four layers, viz., the mass fractions of CFF increases from 0.9%, 1.8%, 2.7% to 3.6%, the average electrical resistivity also decrease progressively from 7.128, 5.818, 2.019 to 0.776 Ω cm. As we know, the cured epoxy has very good electrical insulating properties, its electrical resistivity is about 10^{12}–10^{17} Ω cm. The conductivity of CFF contributes to the high conductive properties of the CFF/SMP composite, and transforms an insulator to a conductor. More layers of CFF will involve more carbon fibers and connections among them, and will form even more conductive paths. With the more conductive paths, more electrons are involved in an electrical circuit. As a result, the composite will have a lower electrical resistivity, and perform a higher electrical heating efficiency under a given voltage.

3.3. Mechanical properties

To investigate the dynamic mechanical properties of pure SMP and CFF/SMP composites at different temperatures, a dynamic thermal scan was conducted to determine the storage modulus and tangent delta using a dynamic mechanical analyzer (Mettler-Toledo AG Analytical, Switzerland). All the specimens with dimensions of 9.0 × 3.0 × 1.0 mm^3 were performed in three-point bending mode at a constant heating rate of 5 °C min^{-1} and an oscillation frequency of 1 Hz from 40 °C to 180 °C.

The curves of storage modulus and tangent delta versus temperature for pure SMP and CFF/SMP composites are plotted in figure 4. It is clear that the addition of CFF increases the storage modulus of the composites over the whole temperature range (figure 4(a)). This is due to the reinforcement of the CFF. The storage modulus decreases sharply within the glass transition region, which shows an excellent variable stiffness property. In figure 4(b), the tangent delta curve of pure SMP approaches the peak value of 0.72 at 97.3 °C, while CFF/SMP composites reach the peak values of 0.32 at 99.6 °C, 0.23 at 99.7 °C, 0.23 at 104.7 °C, and 0.22 at 100.0 °C, respectively. In this study, where the peak value of tangent delta occurs is defined as the glass transition temperature (T_g). It is obvious that the T_g of the pure SMP and CFF/SMP composites are all around 100 °C, which indicates that the incorporation of CFF has little influence on the T_g. However, the peak value of tangent delta decreases greatly after adding the CFF into the SMP resin. The tangent delta is defined as the loss factor, viz. a ratio of loss modulus to storage modulus in viscoelastic materials, and a low tangent delta represents a low internal energy dissipation in dynamic deformations. That is to say, the CFF/SMP composites showing lower tangent delta values possess lower damping properties than pure SMP.

Quasi-static tensile tests were carried out to experimentally demonstrate the mechanical properties of the pure SMP and CFF/SMP composites. The tests were operated on a Zwich/Roell servo-mechanical testing machine with a temperature control box. The dumbbell-shape specimens with different CFF mass fractions (0, 0.9, 1.8, 2.7, 3.6 wt%) were cut form the CFF/SMP plates in accordance with dimensions of type IV specimen (shown in the ASTM standard D638). The quasi-static tensile test were performed at a loading speed of 5 mm min^{-1} within the chamber at three different temperatures, 15 °C (room temperature), 70 °C (about T_g −30 °C), and 130 °C (about T_g +30 °C), respectively.

Five specimens were tested for each sample at each temperature. The average Young's modulus, tensile strength and elongation at break at different temperature are listed in table 1, and standard deviation of each configuration follows '±' sign. Generally, the carbon fibers in the CFFs have much higher Young's modulus, tensile strength, and much lower breaking strain than those of pure SMP. So the improved Young's modulus and tensile strength are obtained by adding the CFFs, and the elongation at break of each specimen decreases along with the addition of CFFs. Comparing three different temperatures, the Young's modulus and tensile strength drop dramatically with the rising temperature, which is consistent with the dynamic mechanical analysis results. The elongation at break of each specimen reaches the highest value at 70 °C (about T_g −30 °C). And when the temperature goes much higher, which is 30 °C above the T_g of the SMP matrix, the specimen is too weak to afford any more deformation, which results in the decrease of breaking strain at 130 °C.

So given both of the electrical properties and mechanical properties, the CFF/SMP composites have tunable electrical resistance, improved strength and stiffness, and considerable elongation. Together, these properties make the CFF/SMP composites superior candidates for morphing structures. Taking the CFF/SMP composite with 2.7 wt% CFF as an

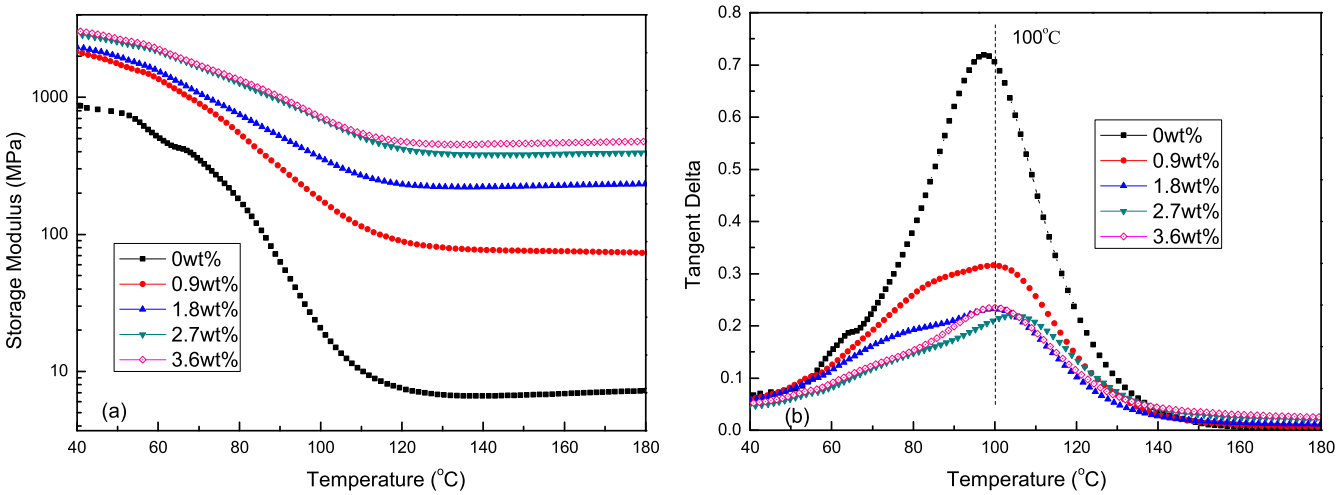

Figure 4. Curves of storage modulus and tangent delta versus temperature of pure SMP and CFF/SMP composite.

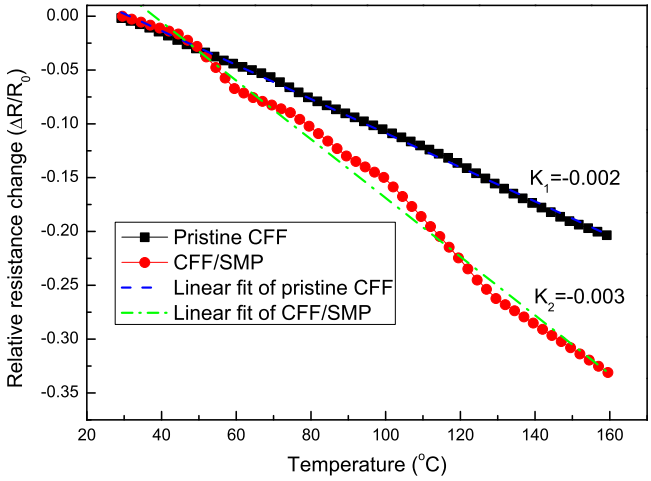

Figure 5. The relative resistance change versus temperature curves for the pristine CFF and CFF/SMP composite with 2.7 wt% filler.

example, we discuss the temperature-strain sensing, shape memory, and heating performances in the sections below.

3.4. Temperature and strain sensing test

As we know, the resistance of the conductive polymer composites can change with the temperature in a certain temperature range. There are two temperature coefficient effects, called positive temperature coefficient effect or negative temperature coefficient (NTC) effect. They depend significantly on the properties of the polymer matrices and the conductive fillers. In this work, the resistance of the conductive filler (CFF) and the conductive composite were monitored from 30 °C to 160 °C. As shown in figure 5, the relative resistance change of both samples are all negative values along with the increasing temperature, indicating that the resistance reduces with the increasing temperature,

Table 1. The average experimental data of the Young's modulus, tensile strength and elongation at break at different temperature.

	0 wt%	0.9 wt%	1.8 wt%	2.7 wt%	3.6 wt%
	Young's modulus (MPa)				
15 °C	1494.42 ± 8.74	1527.45 ± 11.64	1590.28 ± 19.62	1753.58 ± 9.53	2128.10 ± 125.58
70 °C	199.70 ± 30.46	776.19 ± 49.83	816.07 ± 49.83	1068.14 ± 42.73	1363.50 ± ± 42.66
130 °C	16.07 ± 2.97	360.88 ± 44.76	423.01 ± 44.76	752.40 ± 2.42	1094.66 ± 4.49
	Tensile strength (MPa)				
15 °C	64.17 ± 0.55	73.35 ± 5.43	72.28 ± 0.97	82.20 ± 3.20	69.75 ± 4.74
70 °C	18.05 ± 0.21	18.79 ± 0.20	20.10 ± 0.42	28.05 ± 0.78	44.30 ± 1.98
130 °C	2.36 ± 0.40	5.78 ± 0.15	7.30 ± 1.32	14.95 ± 1.20	21.60 ± 0.28
	Elongation at break (%)				
15 °C	5.94 ± 0.39	4.07 ± 0.31	4.03 ± 0.13	3.78 ± 0.15	2.44 ± 0.07
70 °C	39.25 ± 0.07	13.45 ± 1.63	11.79 ± 2.56	6.02 ± 0.13	2.75 ± 0.16
130 °C	16.77 ± 0.25	3.71 ± 1.38	2.30 ± 0.13	2.37 ± 0.16	2.31 ± 0.01

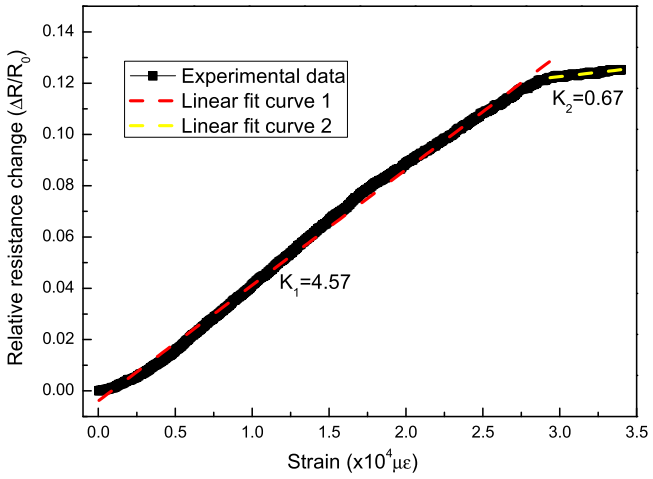

Figure 6. Curves of relative resistance change versus strain in CFF/SMP composite with 2.7 wt% filler.

showing the NTC effect. The relative resistance change of CFF and CFF/SMP composite reach their own minimum −0.204 and −0.331 at the end of the test, 160 °C. This phenomenon could be attributed to the electron movement in the electrical circuit [29]. The electrons in the conductive network pick up additional energy with the increasing temperature, which in return accelerates the electron flow. Then, this accelerated velocity results in a shorter period of cyclic electron flow. Compared with the pure CFF, a more significant resistance decrease is found in the composite at the same temperature. As shown in figure 5, the curves of relative resistance change versus temperature in CFF and CFF/SMP composite are approximately linear in the whole temperature range. The slopes of the linear fitting curves are treated as the sensitivity coefficient, which are −0.002 for the pure CFF and −0.003 for the CFF/SMP composite. The temperature-dependent resistance helps the composite achieve the ability of temperature self-sensing, which means the temperature in the composite can be predicted by monitoring its resistance.

Also, the conductive composite is generally strain sensitive, their electrical resistance changes with the strain altering. The resistance change of the CFF/SMP composite (2.7 wt% CFF) was investigated in a tensile test process until the sample breaking with a constant rate 1 mm min^{-1}. Figure 6 shows curves of the relative resistance change versus strain in the CFF/SMP composite with 2.7 wt% CFF. The resistance increase with the tensile strain. The curve can be linear fitted in two ranges of strain, respectively. In the first region, the specimen undertakes the linear elastic deformation, the resistance increases almost linearly with the strain. This is because the resistance of carbon fiber increase with the tensile strain [30]. In the second region, the change degree of resistance dropped. This results from the strain release induced by the separation of the fibers and resin matrix, and meanwhile the connection between the fibers are partially destroyed. The slope of the linearly fitting curve is treated as the sensing gauge factor, which is 4.57. The period of linear elastic deformation in the first range can be considered as the effective deformation range, where the maximum strain is 2.9×10^4 $\mu\varepsilon$. Hence, the strain-dependent resistance in the CFF/SMP composite with the shape changing ability can predict the deformation level of the composite, which makes the composite deformation self-sensing.

3.5. Shape memory properties

To investigate the shape memory behaviors, the bending test [31] using rectangular strip specimens ($60 \times 10 \times 1$ mm^3) was examined. The specimens were firstly bent into a 'U' shape at 130 °C. In order to minimize the gravity effect, the sample is fixed on a stand in the oven, and the camera is set on top of the oven to get a top view of the shape memory process. The testing of the recovery angle versus time was conducted at 130 °C, namely T_g +30 °C. Figure 7 shows the recovery process of pure SMP and CFF/SMP composite. Figure 8 shows the shape recovery ratio over time. At the temperature of T_g +30 °C, associated with a fast glass transition and strain energy dissipation of the SMP, the SMP and CFF/SMP composite specimens fully deployed. The recovery speed is low within the first 20 s, because it would take a short period of time to completely heat the samples. After that, the samples start to recover faster. It was revealed that the CFF/SMP composite could recover more rapidly with the same recovery ratio (almost 100%) than the pure SMP. It is because the strain energy in the CFF/SMP composite is considered higher than that in the SMP. On the other hand, the CFF could act as a thermal conductive network, which would certainly accelerate the heat transfer within the SMP resin matrix.

As investigation demonstrated above, the CFF/SMP composite with 2.7 wt% CFF have a good electrical and

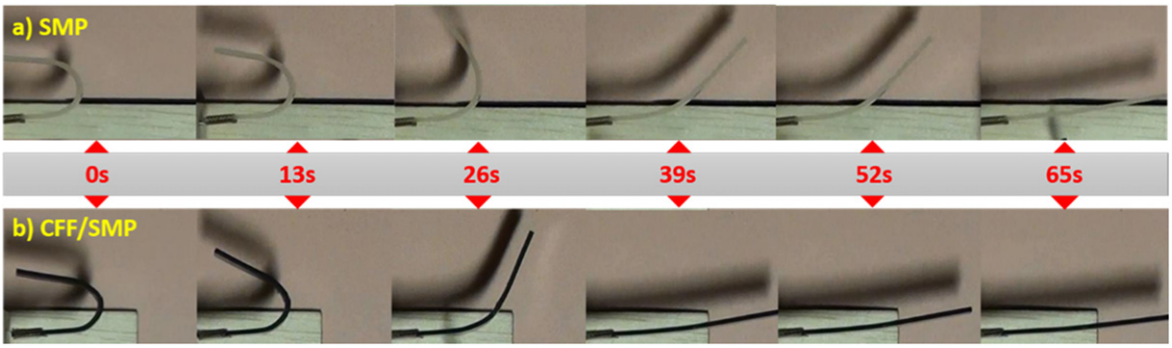

Figure 7. Shape memory process of SMP and CFF/SMP composite (with 2.7 wt% CFF).

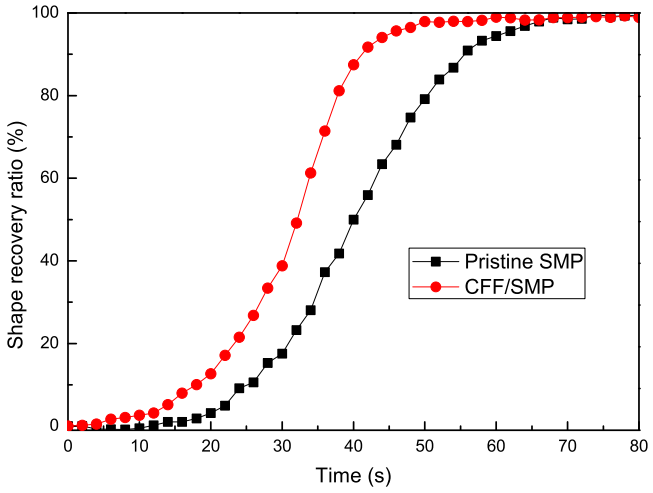

Figure 8. The shape recovery ratio over time.

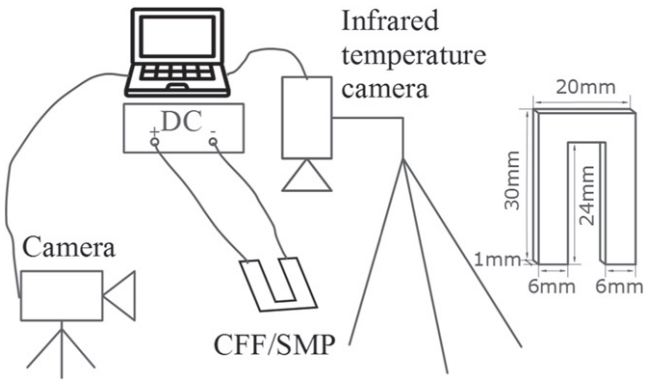

Figure 9. The schematics of the specimens and the test method.

mechanical properties. With the contribution of the CFF, the resistance of the SMP composite is significantly dropped. The transition from an insulator to a conductor makes it is possible to drive a SMP by the electrical resistance heating. This also make the composite obtain the electrical-heating ability. The shape memory composite can be activated without an external heating facility. The electrically triggered shape recovery was investigated using a 'Π' shaped CFF/SMP composite sample. The sample was cut out from a flat composite plate, with the outer dimension of $30 \times 20 \times 1\,mm^3$ and a $24 \times 8\,mm^2$ center gap to form a 'Π' shaped sample. The sample was bent to an 'n' shape at 130 °C, and the shape was fixed by cooling it to room temperature. After that, two electrodes of the CFF/SMP composite sample were connected to a constant 10 V DC power. The recovery process was recorded by a digital camera in front. Meanwhile, the temperature distribution was measured by an infrared temperature camera (VarioCAM® HiRessl, JENOPTIK Infra Tec.) on top. The schematics of the specimens and the test method are shown in figure 9.

The screenshots of the shape recovery process of the CFF/SMP composite sample are shown in figure 10. The whole recovery process takes 15 s. In the first 3 s, the recovery speed is very slow, which means that the sample needs some time to reach the transition temperature of the composite under the Joule heating. After that, the sample starts to recover faster. At about 15 s, the shape recovery process is completed, and no visible deformation is noticed after 15 s. The recovery shape is almost the same with the original flat shape. The temperature distribution along with the shape recovery process was shown in figure 11. The temperature of the specimen increases with the time. The sample started to recover the original shape when the temperature reached the transition temperature after 3 s. The higher temperature ocurred in the region with the higher strain. According to the results of strain sensitivity of the electrical resistance, the electrical resistance increased with the growing strain, so the region undertaken a higher strain has a higher electrical resistance. The higher thermal power appears at the region of the greater electrical resistance in a series circuit. The high shape recovery speed and ratio in this test indicates the CFF/SMP composite can be a potential raw material for electrical-heating and self-activated morphine structure.

3.6. Heating performance

The previous researches about the conductive SMP composite's electrical heating properties mostly concentrated in the sample with a small area like the sample mentioned in the electrically induced shape recovery test. However, in order to make an electrical-heating morphing structure or use in other engineering applications, the electrical heating properties should be explored with samples with a relatively large area. The CFF/SMP composite containing 2.7 wt% CFF was manufactured with the dimension of $120 \times 65 \times 1\,mm^3$. The temperature distribution was measured by an infrared temperature camera (VarioCAM® HiRessl, JENOPTIK Infra Tec.). Figure 12 shows the surface temperature distribution along with the heating time under a 25 V DC power. The surface temperature increased with the heating time, and an equilibrium temperature distribution of about 130 °C was achieved at 70 s. The temperature distribution was uniform as shown in the snapshots, due to the uniform conductive network. Therefore, the CFF/SMP composite will be a promising candidate for the morphing structures with the uniformly electrical-heating property, low cost, and simple manufacture process.

Furthermore, the average surface temperature was tested under the voltage from 5 to 30 V with a constant interval of 5 V, corresponding to the heat flux densities $180\,W\,m^{-2}$, $725\,W\,m^{-2}$, $1779\,W\,m^{-2}$, $3653\,W\,m^{-2}$, $5176\,W\,m^{-2}$, and $9676\,W\,m^{-2}$, respectively. The temperature rising process, the equilibrium temperature, and the heating rate were demonstrated in figure 13. In this study, the heating rate is defined as the ratio of the equilibrium temperature to the time it takes. When the heat flux density is no more than $5176\,W\,m^{-2}$, the equilibrium temperature and heating rate increase with the increasing heat flux densities. And in this situation, the CFF/SMP composite's temperature could reach equilibrium at 27 °C, 41 °C, 66 °C, 98 °C, and 134 °C within 25 s, 32 s, 42 s, 55 s, and 70 s, respectively. When the flux density is $9676\,W\,m^{-2}$, the surface temperature increased vigorously in the beginning and then decreased, and the

Figure 10. Screenshots of the shape recovery process of the CFF/SMP composite sample (front view).

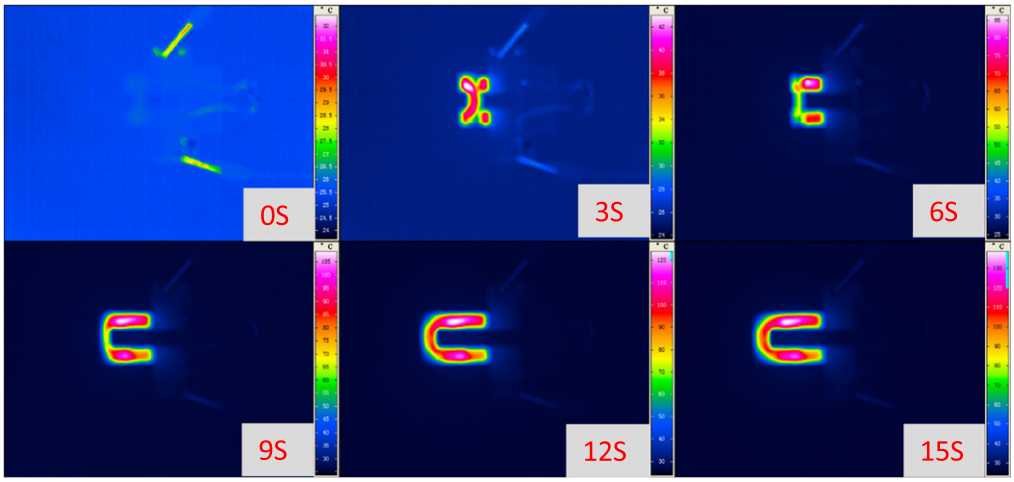

Figure 11. Snapshots of shape recovery and temperature distributions of CFF/SMP composite sample (top view).

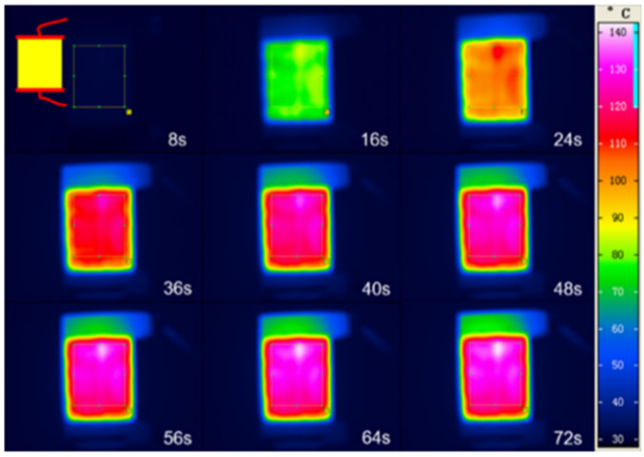

Figure 12. Snapshots of the surface temperature distributions of CFF/SMP composite sample.

sample burned with smoke in the end. This is because the resin matrix has a low thermal decomposition temperature and a low thermal conductivity. The resin would decompose and burn under a severe thermal shock. As a result, the heat flux density applied to the composite should be coordinated with the service conditions including the thermal convection and thermal conduction. If the conditions count against the heat loss, a lower heat flux density can heat the composite soon. An extremely high heat flux density should be avoided in case of the decomposition of the resin. Otherwise, a higher heat flux density should be applied if the condition is conducive to heat loss like the actual flight condition.

As we know, the laminates are a major category in the composite field. The lamination can tailor the directional dependence of strength and stiffness of a composite material to match the loading environment [32]. Laminates can uniquely suit to their objectives owing to the adjustable number and direction of each layer according to the requirement. Similar to the laminates, not merely the strength and stiffness but also the temperature distribution of the CFF/SMP composite can be tailored by designing the lamination of CFF. The resistance distribution determined the heating power distribution under a given voltage or current. In a series circuit, the heating prower is proportional to the resistance. A higher heating power is obtained where more layers of CFF were incorporated. In a parallel circuit, the heating prower is

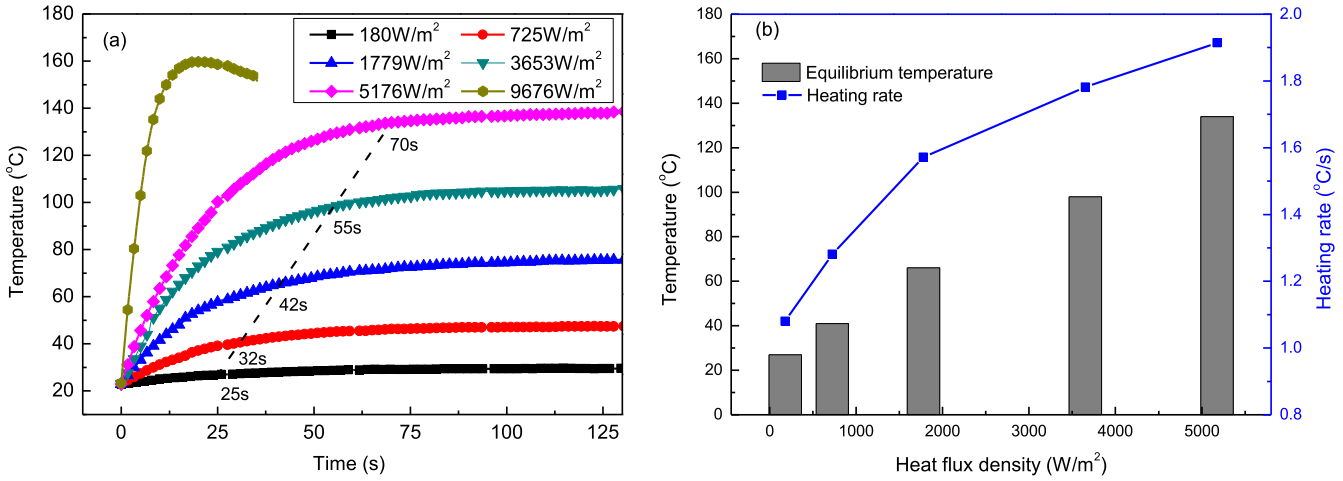

Figure 13. (a) The electric heating process curves of the sample surface at different heat flux densities. (b) The equilibrium temperature and heating rate at different heat flux densities.

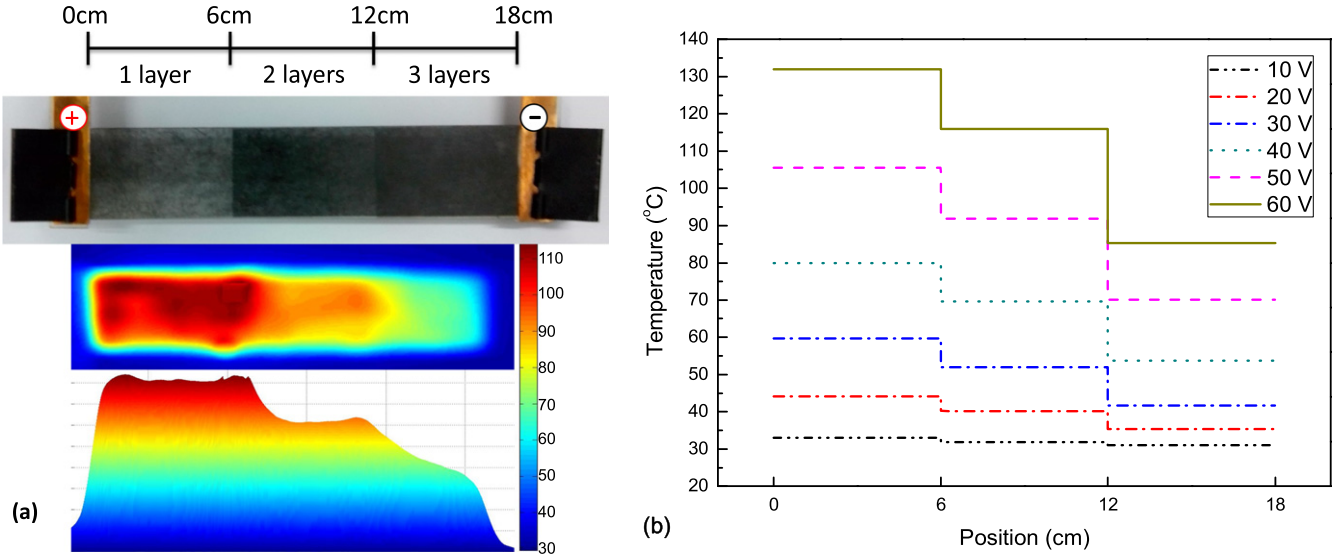

Figure 14. (a)The temperature distribution of a CFF/SMP laminate, (b) the average temperature of each district in the laminate under different voltages.

inversely proportional to the resistance. In this section, a specimen with different layers in different districts was prepared. In the three consecutive districts from left to right, the laminate contains 1, 2, and 3 layers of CFF at each district, respectively. Figure 14(a) shows the temperature distribution of different districts under a 50 V DC power. In this circuit, this three districts can be treated as three series resistors, and the higher heating power can be performed where the bigger resistance achieves, i.e., where less layers of CFF is incorporated. Consequently, we observed a ladder-like temperature distribution on the surface of the CFF/SMP composite. The temperature decreases with the increasing number of layers. The average temperatures observed under different voltages are shown in figure 14(b). As we operated all the tests in the series circuit, the highest average temperature appears at the distinct with 1 layer CFF, and the difference is more significant as the valtage increases from 10 to 60 V. Thus it can be seen that the laminated conductive CFFs give great design space and manufacturing flexibility of the CFF/SMP composite for morphing structures.

4. Conclusions

This work demonstrates a systematic research of the electrical property, mechanical property and heating property of an electrical-heating and self-sensing shape memory composites incorporated with the CFFs. The composite gives a low electrical resistivity due to the conductive network introduced by the CFF. The electrical resistivity could be as low as 0.776 Ω cm when the mass fraction is 3.6%. The Young's modulus and strength are greatly enhanced compared with the pure SMP. Although the elongation at break decreases after adding the CFF, it can still meet the requirement of the variable camber morphing. The temperature sensing, strain sensing and electrical triggered shape memory properties

make the composite a self-sensing and self-active material. The temperature sensitivity coefficient and the strain gauge factor of the composite are −0.003 and 4.57, respectively. The composite shape recovery can be triggered by self-heating within 15 s without an external heater. The composite not only can be uniformly electrical-heated with a uniform laminates, but also has the design flexibility of temperature distribution by incorporating different layers of CFFs in different place. Considering all these features, the CFF/SMP composite can be a promising candidate for the self-sensing and electrical-heating morphing structure with low cost and simple manufacture process.

Acknowledgments

This work is supported by the National Natural Science Foundation of China: Grant No. 11225211.

References

[1] Behl M and Lendlein A 2007 Shape-memory polymers *Mater. Today* **10** 20–8
[2] Ratna D and Karger-Kocsis J 2008 Recent advances in shape memory polymers and composites: a review *J. Mater. Sci.* **43** 254–69
[3] Gall K, Kreiner P, Turner D and Hulse M 2004 Shape-memory polymers for microelectromechanical systems *J. Microelectromech. Syst.* **13** 472–83
[4] Liu Y J, Lv H B, Lan X, Leng J S and Du S Y 2009 Review of electro-active shape-memory polymer composite *Compos. Sci. Technol.* **69** 2064–8
[5] Perkins D A, Reed J L and Havens E (ed) 2004 Morphing wing structures for loitering air vehicles *45th AIAA Structures, Structural Dynamics and Materials Conf.*
[6] Bye D R and McClure P D (ed) 2007 Design of a morphing vehicle *48th AIAA Structures, Structural Dynamics, and Materials Conf.*
[7] Lan X, Liu Y, Lv H, Wang X, Leng J and Du S 2009 Fiber reinforced shape-memory polymer composite and its application in a deployable hinge *Smart Mater. Struct.* **18** 024002
[8] Deng H, Lin L, Ji M, Zhang S, Yang M and Fu Q 2014 Progress on the morphological control of conductive network in conductive polymer composites and the use as electroactive multifunctional materials *Prog. Polym. Sci.* **39** 627–55
[9] Meng H and Hu J L 2010 A brief review of stimulus-active polymers responsive to thermal, light, magnetic, electric, and water/solvent stimuli *J. Intell. Mater. Syst. Struct.* **21** 859–85
[10] Meng H and Li G 2013 A review of stimuli-responsive shape memory polymer composites *Polymer* **54** 2199–221
[11] Cho J W, Kim J W, Jung Y C and Goo N S 2005 Electroactive shape-memory polyurethane composites incorporating carbon nanotubes *Macromol. Rapid Commun.* **26** 412–6
[12] Koerner H, Price G, Pearce N A, Alexander M and Vaia R A 2004 Remotely actuated polymer nanocomposites—stress-recovery of carbon-nanotube-filled thermoplastic elastomers *Nat. Mater.* **3** 115–20
[13] Sahoo N G, Jung Y C and Cho J W 2007 Electroactive shape memory effect of polyurethane composites filled with carbon nanotubes and conducting polymer *Mater. Manuf. Process.* **22** 419–23
[14] Yoo H J, Jung Y C, Sahoo N G and Cho J W 2006 Polyurethane-carbon nanotube nanocomposites prepared by *in situ* polymerization with electroactive shape memory *J. Macromol. Sci.* B **45** 441–51
[15] Tang Z H, Kang H L, Wei Q Y, Guo B C, Zhang L Q and Jia D M 2013 Incorporation of graphene into polyester/carbon nanofibers composites for better multi-stimuli responsive shape memory performances *Carbon* **64** 487–98
[16] Schmidt A M 2006 Electromagnetic activation of shape memory polymer networks containing magnetic nanoparticles *Macromol. Rapid Commun.* **27** 1168–72
[17] Leng J, Lv H, Liu Y and Du S 2007 Electroactivate shape-memory polymer filled with nanocarbon particles and short carbon fibers *Appl. Phys. Lett.* **91** 144105
[18] Leng J S, Lan X, Liu Y J and Du S Y 2009 Electroactive thermoset shape memory polymer nanocomposite filled with nanocarbon powders *Smart Mater. Struct.* **18** 074003
[19] Tang Z H, Sun D Q, Yang D, Guo B C, Zhang L Q and Jia D M 2013 Vapor grown carbon nanofiber reinforced bio-based polyester for electroactive shape memory performance *Compos. Sci. Technol.* **75** 15–21
[20] Buckley P R *et al* 2006 Inductively heated shape memory polymer for the magnetic actuation of medical devices *IEEE Trans. Biomed. Eng.* **53** 2075–83
[21] Leng J, Huang W, Lan X, Liu Y and Du S 2008 Significantly reducing electrical resistivity by forming conductive Ni chains in a polyurethane shape-memory polymer/carbon-black composite *Appl. Phys. Lett.* **92** 204101
[22] Lu H B and Gou J H 2012 Fabrication and electroactive responsive behavior of shape-memory nanocomposite incorporated with self-assembled multiwalled carbon nanotube nanopaper *Polym. Adv. Technol.* **23** 1529–35
[23] Kwok N and Hahn H T 2007 Resistance heating for self-healing composites *J. Compos. Mater.* **41** 1635–54
[24] Sahoo N G, Jung Y C, Goo N S and Cho J W 2005 Conducting shape memory polyurethane-polypyrrole composites for an electroactive actuator *Macromol. Mater. Eng.* **290** 1049–55
[25] Casado U M, Quintanilla R M, Aranguren M I and Marcovich N E 2012 Composite films based on shape memory polyurethanes and nanostructured polyaniline or cellulose–polyaniline particles *Synth. Met.* **162** 1654–64
[26] Abry J C, Bochard S, Chateauminois A, Salvia M and Giraud G 1999 *In situ* detection of damage in CFRP laminates by electrical resistance measurements *Compos. Sci. Technol.* **59** 925–35
[27] Leng J, Wu X and Liu Y 2009 Effect of a linear monomer on the thermomechanical properties of epoxy shape-memory polymer *Smart Mater. Struct.* **18** 095031
[28] Bauhofer W and Kovacs J Z 2009 A review and analysis of electrical percolation in carbon nanotube polymer composites *Compos. Sci. Technol.* **69** 1486–98
[29] Lu H B, Yin W L, Huang W M and Leng J S 2013 Self-assembled carboxylic acid-functionalized carbon nanotubes grafting onto carbon fiber for significantly improving electrical actuation of shape memory polymers *Rsc Adv.* **3** 21484–8
[30] Zheng L, Li Z, Song X and Lü Y 2008 Effect of strain on the electrical resistance of continuous carbon fiber monofilament *J. Funct. Mater.* **39** 440–2
[31] Xie F, Huang L, Liu Y and Leng J 2014 Synthesis and characterization of high temperature cyanate-based shape memory polymers with functional polybutadiene/acrylonitrile *Polymer* **55** 5873–9
[32] Jones R M 1975 *Mechanics of Composite Materials* (New York: McGraw-Hill)